FATIGUE LIFE PREDICTION OF BRIDGES CONSIDERING THE EFFECT OF MULTIAXIAL STRESSES

M. OHGA[1*], K. KARUNANANDA[1], P.B.R. DISSANAYAKE[2] and A.M.N.D. ADASOORIYA[1]

[1]Department of Civil and Environmental Engineering, Ehime University, Japan

[2]Department of Civil Engineering, University of Peradeniya, Sri Lanka

ABSTRACT

This paper presents a new low cycle fatigue model to predict life of steel bridges. It consists of Coffin-Manson strain-life curve with a new strain based damage index. The damage variable is based on a modified von Mises equivalent strain to account for effects of loading non-proportionality and strain path orientation in low cycle multiaxial stress state. The proposed model was verified by comparing with experimental test results of two materials. Then, it was applied an existing riveted wrought iron railway bridge to estimate fatigue life due to usual traffic and earthquake loadings. The obtained results verify the importance and effectiveness of the proposed model over commonly used Miner's rule model in fatigue life estimation of steel bridges.

Keywords: High cycle fatigue, Low cycle fatigue, Steel bridges, Life prediction, Earthquake loading.

5. Introduction

High cycle fatigue (HCF) caused by low amplitude traffic loading is one of the main safety considerations of steel bridges. In addition, there are certain situations that a bridge may be subjected to high amplitude loading such as earthquake or unexpected stress concentrations during its service life. When such an event occurs, some members may undergo inelastic stresses. These inelastic stresses may cause low cycle fatigue (LCF) damage during the high amplitude loading while subjecting to HCF in service conditions. This combined damage of HCF and LCF may be a reason for a much reduced life (Kondo and Okuya 2007).

The von Mises equivalent strain and Coffin-Manson strain-life curve are used with Miner's rule as the general method to estimate the life for LCF conditions (Suresh 1998). The Miner's rule is the simplest and the most widely used fatigue life prediction technique. One of its interesting features is that life calculation is simple and reliable when the detailed loading history is unknown. However under many variable amplitude loading conditions, Miner's rule based life predictions have been found to be unreliable since it cannot capture loading sequence effect (Siriwardane et al. 2008). Further, von Mises equivalent strain cannot capture the effects due to non-proportional loading and orientation of strain path which are the key features of multiaxial LCF stress state (Borodii and Strizhalo 2000). von Mises strain generally predicts a lesser strain value than the actual strain of the material that undergoes. Due to these reasons, LCF life estimation by Miner's rule based model may be inaccurate in multiaxial variable amplitude loading. Therefore, it is

*Corresponding author, Tel/Fax: +81-89-927-9816, E-mail: ohga@cee.ehime-u.ac.jp

necessary to have a different model, which is based on commonly available material properties, to estimate more accurately the life for LCF due to variable amplitude loading.

The objective of this paper is to propose a new model to accurately estimate the LCF life (crack initiation life) due to a high amplitude loading. Initially, the proposed model is presented and then the verification of the proposed model is discussed. Finally, the proposed model is applied to an existing wrought iron railway bridge to estimate fatigue life.

6. Proposed fatigue model

This section proposes the new low cycle fatigue model to estimate life of steel structures. Initially, the details relevant to proposed damage variable, Coffin-Manson strain-life fatigue curve are discussed. Finally, it clearly describes the proposed damage indicator.

6.1. Damage variable

The proposed damage variable for low cycle multiaxial stress state is given as (Borodii and Strizhalo 2000),

$$\varepsilon_{eq} = (1+\alpha\phi)(1+kSin\varphi)\varepsilon_{VM} \tag{1}$$

where ε_{eq} is the equivalent strain amplitude in multiaxial stress state, α is the material parameter for loading non-proportionality, ϕ is the cycle non-proportionality parameter, k is the material parameter for strain path orientation, φ is the angle measured from the principal direction to the applied strain path and ε_{VM} is the von Mises equivalent strain as given,

$$\varepsilon_{VM} = \frac{1}{(\sqrt{2}\times(1+\nu))}\left[(\varepsilon_{xx}-\varepsilon_{yy})^2+(\varepsilon_{yy}-\varepsilon_{zz})^2+(\varepsilon_{zz}-\varepsilon_{xx})^2+\frac{3}{2}\times(\gamma_{xy}^2+\gamma_{yz}^2+\gamma_{zx}^2)\right]^{1/2} \tag{2}$$

where ν is the Poisson's ratio. ε and γ are the axial and shear strain amplitudes in respective planes.

The first expression in parentheses of Eq. (1) is the degree of additional strain hardening depending on the cycle geometry (to account for non-proportional loading). The second expression in parentheses is strain hardening depending on the orientation of the cyclic strain path (proportional loading). The material parameters (α and k) have to be estimated by additional testing of the material. ϕ and φ can be estimated for given strain path considering cycle geometry and its orientation, respectively (Borodii and Strizhalo 2000).

The parameter, φ, is estimated by the orientation of the applied strain path (measured angle) with respect to the principal direction. The principal direction of a material is the direction that gives the highest live and usually it is the torsion axis for most of materials. However, this parameter does not represent the characteristics of material and presented by the parameter, k. The parameter, k, is estimated by at least three fatigue tests. In fact, the parameters, k and φ, collectively represent the effect of proportional loading.

The parameter, ϕ, is estimated from the ratio of areas of a given non-proportional cycle path to a circular cycle path. As this parameter is related to cycle geometry, a different parameter is necessary to represent material characteristics. It is represented by the parameter, α, and three fatigue tests are necessary to estimate the parameter, α. These two parameters (α,ϕ) collectively represent the effect of non-proportional loading.

6.2. Strain-life curve

The strain-life curve used in this study is the Coffin-Manson relationship as given,

$$\varepsilon_{eq} = \frac{\sigma_f^{'}}{E}(2N)^b + \varepsilon_f^{'}(2N)^c \tag{3}$$

where ε_{eq} is the equivalent strain amplitude in multiaxial stress state, N is the number of cycles to failure, $\sigma_f^{'}$ is the fatigue strength coefficient, b is the fatigue strength exponent, $\varepsilon_f^{'}$ is the fatigue ductility coefficient, c is the fatigue ductility exponent and E is the elastic modulus of the material.

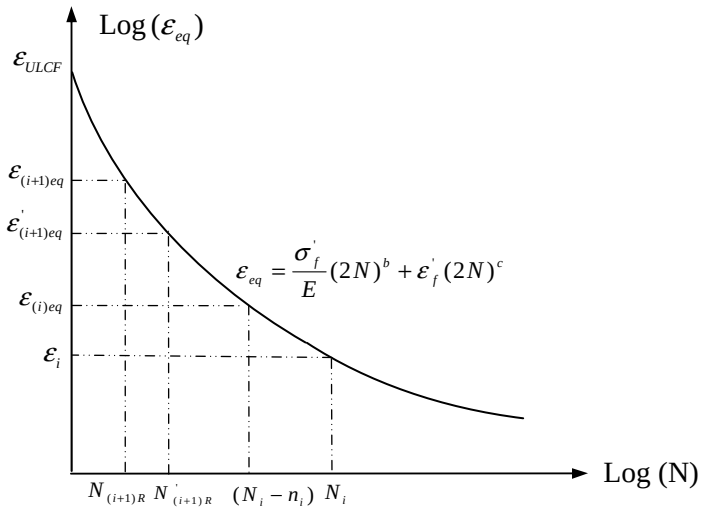

Figure 1: Schematic representation of the Coffin-Manson strain-life curve

The ultimate strain of low cycle fatigue $(\varepsilon)_{ULCF}$ which is the strain amplitude corresponding to failure in half reversal (a quarter of a cycle) is obtained from Eq. (3) as,

$$(\varepsilon)_{ULCF} = \varepsilon_f^{'} \tag{4}$$

Most of pure metals and alloys, fatigue properties are available in the literature and therefore corresponding Coffin-Manson strain-life curve can be obtained easily.

6.3. Damage indicator

The proposed damage indicator considers damage of LCF due to variable amplitude loading. Consider, a component is subjected to a certain equivalent strain amplitude of $(\varepsilon)_i$, n_i number of cycles at load level i, N_i is the fatigue life (number of cycles to failure) corresponding to $(\varepsilon)_i$ (Figure 1). Therefore, the reduced life at the load level i is obtained as $(N_i - n_i)$. The damage equivalent strain $(\varepsilon)_{(i)eq}$ (Figure 1), corresponding to the failure life $(N_i - n_i)$ is defined as i^{th} level damage equivalent strain. Then, the new damage indicator, D_i is stated as,

$$D_i = \frac{(\varepsilon)_{(i)eq} - (\varepsilon)_i}{(\varepsilon)_u - (\varepsilon)_i} \quad (5)$$

where the $(\varepsilon)_u$ is given in Eq. (4)

At the end of i^{th} loading level, damage D_i has been accumulated (occurred) due to the effect of $(\varepsilon)_{i+1}$ loading cycles, the damage (same damage given in Eq. 5) is transformed to load level *i+1* as below.

$$D_i = \frac{(\varepsilon)'_{(i+1)eq} - (\varepsilon)_{i+1}}{(\varepsilon)_u - (\varepsilon)_{i+1}} \quad (6)$$

Then, $(\varepsilon)'_{(i+1)eq}$ is the damage equivalent strain at loading level *i+1* and it is calculated from Eq. (6) as,

$$(\varepsilon)'_{(i+1)eq} = D_i[(\varepsilon)_u - (\varepsilon)_{i+1}] + (\varepsilon)_{i+1} \quad (7)$$

The corresponding equivalent number of cycles to failure $N'_{(i+1)R}$ is obtained from the strain-life curve as shown in Figure 1. The $(\varepsilon)_{i+1}$ is the strain at the level *i+1* and supposing that it is subjected to $n_{(i+1)}$ number of cycles, then the corresponding residual life at load level *i+1*, $N_{(i+1)R}$ is calculated as,

$$N_{(i+1)R} = N'_{(i+1)R} - n_{(i+1)} \quad (8)$$

Therefore, strain, $(\varepsilon)_{(i+1)eq}$ which corresponds to $N_{(i+1)R}$ at load level *i+1*, is obtained from the strain-life curve as shown in Figure 1. Then the cumulative damage at the end of load level *i+1* is defined as,

$$D_{(i+1)} = \frac{(\varepsilon)_{(i+1)eq} - (\varepsilon)_{i+1}}{(\varepsilon)_u - (\varepsilon)_{i+1}} \quad (9)$$

This procedure is carried out until D_i is equal to 1. The proposed damage indicator calculation is shown in the flow chart given in Figure 2.

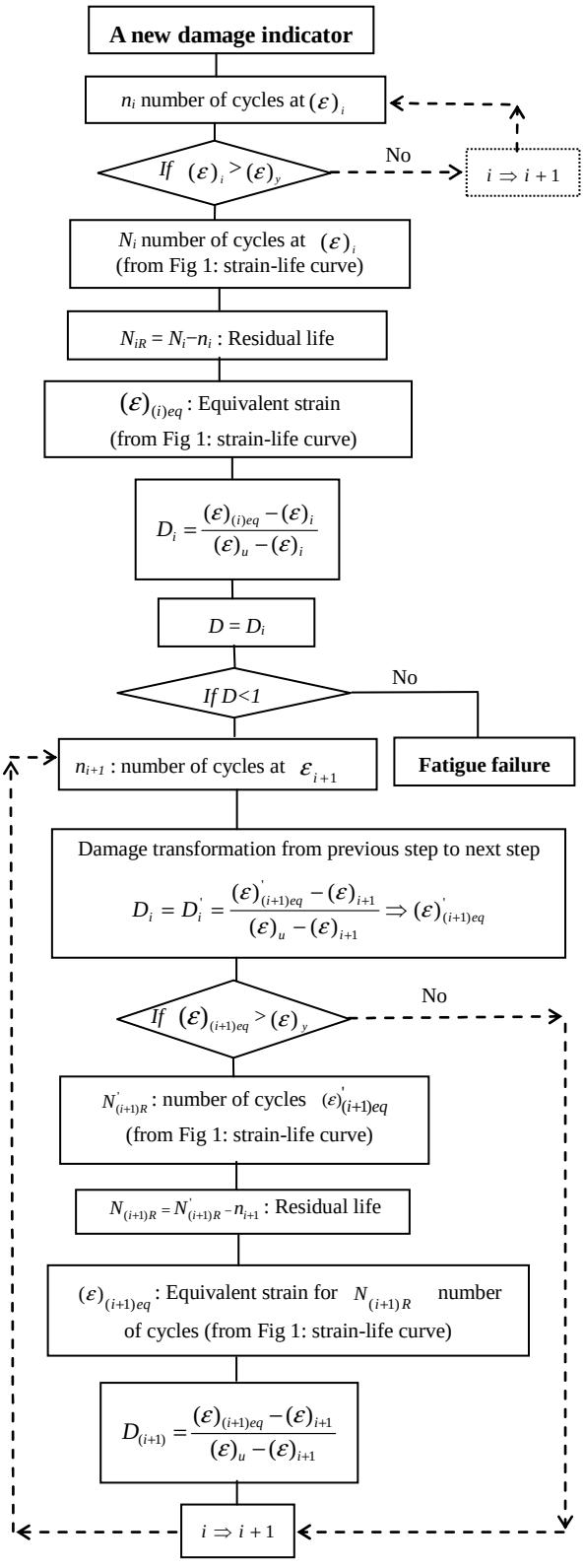

Figure 2: Flow chart of the proposed damage indicator

7. Verification of the proposed model

This section explains the verification of the proposed LCF model by comparing experimental fatigue test results of two materials which were obtained from the literature. Two materials are pure titanium and S304 stainless steel. During these tests, axial (A), torsional (T), in-phase (I) and 90^o -out- of-phase (O) loadings were used in different sequences. Strain variations of strain-controlled fully reversed axial, torsional, in- phase and out-of-phase loadings are shown in Figure 3.

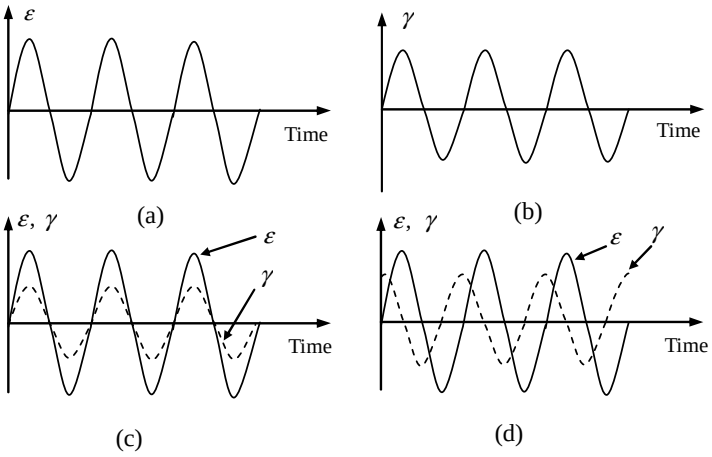

Figure 3: Strain variations for (a) axial loading; (b) torsional loading; (c) in-phase loading; (d) 90^o -out-of-phase loading

7.1. Verification for Pure Titanium

Block loading fatigue tests performed by Shamsaei et al. 2010 were used verify the proposed fatigue model. In the block loading test, axial (A), torsional (T), 90^o -out-of-phase (O) loadings were applied in different combinations as shown in Table 1. Applied wave forms were sinusoidal as shown in Figure 3.

Table 1 Experimental summary and predicted fatigue lives of pure Titanium

Test	First load level		Second load level		Experimental life (cycles)	Predicted life (cycles)	
	von Mises Strain amplitude	No of cycles (n_1)	von Mises Strain amplitude	No of cycles (n_2)		Previous model	Proposed model
AA1	0.0070	491	0.0110	214	705	808	873
AA2	0.0110	104	0.0070	302	406	1399	1073
AA3	0.0110	200	0.0070	186	386	1133	743
TT1	0.0073	1115	0.0113	242	1357	1270	1373
TT2	0.0113	198	0.0073	805	1003	1155	770
AT	0.0090	228	0.0093	397	625	766	761
TA	0.0093	434	0.0090	375	809	763	767
AO	0.0090	228	0.0112	235	463	497	530
OA	0.0112	138	0.0090	155	293	620	536
OT	0.0112	138	0.0093	467	605	635	544
TO	0.0093	428	0.0112	520	683	600	648
TAOTOA	Strain amplitudes = 0.0073, 0.0070, 0.0088, 0.0073, 0.0088, 0.0070		Each loading mode with number of cycles = 50		1050 (3.5 blocks)	1160	1158

Further, authors (Shamsaei et al. 2010) have published constant amplitude fatigue test results. From that, parameters, k and α are estimated as 0.04 and 0.08, respectively. Fatigue lives were predicted using the proposed and previous models as given in Table 1.

Percentage variations of predictions from experimental results were estimated for previous and proposed models. The previous model has a percentage variation of 27.7 % while the proposed model has a value of 17.7 %. Therefore, the proposed model based fatigue lives are more accurate than previous model predictions for the pure titanium.

7.2. Verification for S304 steel

Fatigue tests performed by Chen et al. 2006 were used verify the proposed fatigue model. Axial (A) torsional (T), in-phase (I) and 90^o-out-of-phase (O) loadings have been applied in different sequences. Applied wave forms of axial and torsional loadings were triangular and in-phase and 90^o out-of phase loadings were sinusoidal as shown in Figure 3. Parameters, k and α, were obtained as 0.20 and 0.80, respectively (Borodii 2007). Fatigue lives were predicted using the proposed and previous models as given in Table 2.

Table 2 Experimental summary and predicted fatigue lives of S304 stainless steel

Test	First load level		Second load level		Experimental life (cycles)	Predicted life (cycles)	
	von Mises strain amplitude	No of cycles (n_1)	von Mises strain amplitude	No of cycles (n_2)		Previous model	Proposed method
AT1	0.006	973	0.006	2994	3967	5321	4891
AT2	0.006	1946	0.006	981	2927	4474	3998
IO1	0.0057	1228	0.0057	1053	2281	2518	2578
IO2	0.0057	1965	0.0057	1225	3190	3122	3209
IO3	0.0057	2456	0.0057	687	3143	3525	3629
IO4	0.0057	3685	0.0057	549	4234	4532	4671
OI1	0.0057	364	0.0057	3572	3936	6726	5345
OI2	0.0057	583	0.0057	2574	3157	5732	4139
OI3	0.0057	728	0.0057	2481	3209	5073	3448
OI4	0.0057	1093	0.0057	2165	3258	3416	2157
TA1	0.006	1559	0.006	1310	2869	4022	4052
TA2	0.006	3117	0.006	825	3942	4748	4821
TA3	0.006	4676	0.006	368	5044	5474	5505

The percentage variations of predictions from the experimental results were estimated for the previous and proposed models as 11.3 and 6.9 %, respectively. Therefore, the proposed model based predicted fatigue lives are more accurate than previous model predictions for S304.

8. Case study: fatigue life estimation of a bridge member

The proposed method was applied to find the fatigue life of a wrought iron railway bridge member. The

selected bridge (Figure 4a) is one of the longest railway bridges in Sri Lanka located near Colombo and the considered member is shown in Figure 4b (Siriwardane et al. 2008). The evaluations are especially based on secondary stresses and strains, which are generated around the riveted connection of the member due to stress concentration effect of primary stresses caused by usual traffic and earthquake loadings. Schematic representation of primary and secondary stress areas of the considered member is given in Figure 4(c).

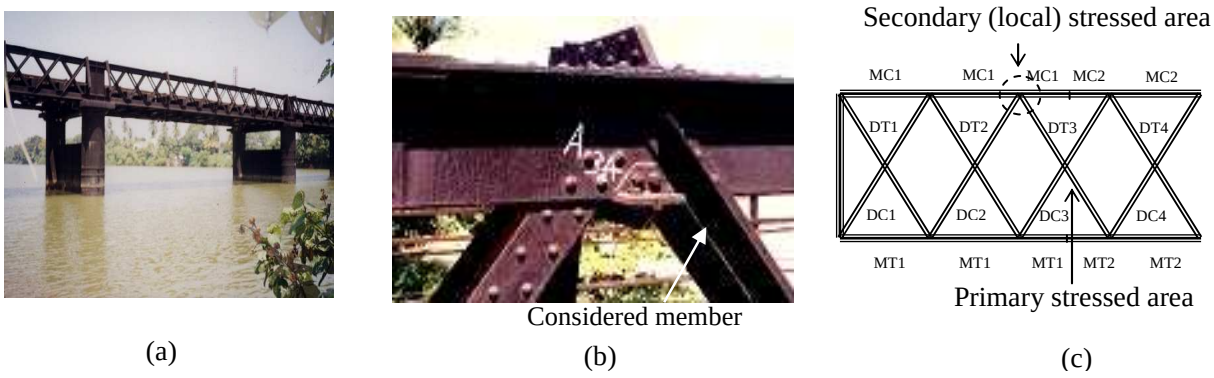

Fig. 4. Views of (a) the bridge; (b) considered member; (c) schematic representation of the critical member and related areas for primary and local stresses

The damage due to LCF is evaluated based on the state of strain when all rivets are active (tight rivets) while they have no clamping force. The clamping force is generally defined as the compressive force in the plates which is induced by the residual tensile force in the rivet. Since this study assumes that the riveted locations have no clamping force (value of clamping force is zero), the connected members are considered to subject to the biaxial stress state. Therefore, a critical member without rivets can be considered to analyze the biaxial state of stress of a 2D finite element analysis. The nine node isoperimetric shell elements were used for the FE analysis.

Earthquake is considered to occur at different times (10, 50, 75 and 100 years) of the bridge life. It is assumed that usual traffic load is followed after the earthquake. The fatigue damages due to earthquake and usual traffic loadings were estimated using the proposed model and the HCF model given in Siriwardane et al. (2008), respectively. Obtained fatigue lives are given in Table 3 (column 4). In addition, the previous model (Coffin-Manson curve with the Miner's rule) was also used in life estimation and the corresponding results are given in Table 3 (column 2).

Table 3 Fatigue life of the member for different earthquake occurrences

Time of earthquake* (years)	Previous model (Miner's rule)		Proposed model	
	Fatigue life (years)	Percentage reduction of life (%)	Fatigue life (years)	Percentage reduction of life (%)
10	127.7	5.0	148.5	8.8
50	127.7	5.0	120.5	26.0
75	127.7	5.0	145.1	10.9
100	127.7	5.0	159.9	1.8
No earthquake	134.5	-	162.8	-

*After construction

The results indicate that LCF damage by earthquake loading causes a considerable reduction of bridge life. For the proposed model, percentage reduction of life is higher when the earthquake occurs at the 50 years compared to those occurring in other times. The relative amplitude difference between traffic and earthquake loadings determines the year at which maximum fatigue life is reduced. For the previous model, the reduction of service life is constant irrespective of time of earthquake occurrence. Comparison of fatigue life reveals that the proposed model predictions differ from the previous model predictions.

The obtained results verifies that the Coffin-Manson strain-life curve with new damage indicator better represents LCF damage than the Coffin-Manson relationship with Miner's rule. The differences of case study results confirm the importance of accurate LCF model to estimate the fatigue life of existing steel bridges.

9. Conclusions

A LCF model was proposed to predict the fatigue life of bridges due to high amplitude loading. A verification of the model was conducted by comparing the predicted lives with experimental lives of two materials. It was shown that the proposed fatigue model gives a more accurate fatigue life for damage of LCF situations where detailed stress histories are known. The proposed fatigue model was utilized to estimate the fatigue life of a bridge member. Case study realized the importance and effectiveness of considering the earthquake induced LCF damage in addition to HCF damage due to usual traffic loading in steel bridges.

6. Acknowledgement

The authors wish to express their sincere gratitude to Professor M.P Ranaweera and the team of experts who worked in the Sri Lankan Railway Bridge project, for their great advice in carrying out this research.

References

Borodii MV (2007). Life calculation for materials under irregular nonproportional loading, Strength of Materials, 39(5), pp. 560-565.

Borodii MV and Strizhalo VA (2000). Analysis of experimental data on a low cycle fatigue under nonproportional strain hardening, International Journal of Fatigue, 22(4), pp. 275-282.

Chen X, Jin D and Kim KS (2006). Fatigue life prediction of type 304 stainless steel under sequential biaxial loading, International Journal of Fatigue, 28(3), pp. 289-299.

Kondo Y and Okuya K (2007). The effect of seismic loading on the fatigue strength of welded joints. Material Science and Engineering A. 468-470. pp. 223-229.

Shamsaei, N, Galdskyi M, Panasovskyi K, Shukaev S and Fatemi A (2010). Multiaxial fatigue of Titanium including step loading and load path alteration and sequence effects, International Journal of Fatigue, 32(11), pp. 1862-1874.

Siriwardane S, Ohga M, Dissanayake R and Taniwaki K (2008). Application of new damage indicator-based sequential law for remaining fatigue life estimation of railway bridges. Journal of Constructional Steel Research. 64(2). pp. 228-237.

Suresh S (1998). Fatigue of Materials, UK: Cambridge University Press, Cambridge.